Lab on a Chip



PAPER

View Article Online



Cite this: Lab Chip, 2022, 22, 121

Lymphangion-chip: a microphysiological system which supports co-culture and bidirectional signaling of lymphatic endothelial and muscle cells†

Amirali Selahi, Da Teshan Fernando, Sanjukta Chakraborty, b Mariappan Muthuchamy, b David C. Zawieja and Abhishek Jain ** ** David C. Zawieja and Abhishek Jain ** David C. Zawieja and C. Zawieja and

The pathophysiology of several lymphatic diseases, such as lymphedema, depends on the function of lymphangions that drive lymph flow. Even though the signaling between the two main cellular components of a lymphangion, endothelial cells (LECs) and muscle cells (LMCs), is responsible for crucial lymphatic functions, there are no in vitro models that have included both cell types. Here, a fabrication technique (gravitational lumen patterning or GLP) is developed to create a lymphangion-chip. This organ-on-chip consists of co-culture of a monolayer of endothelial lumen surrounded by multiple and uniformly thick layers of muscle cells. The platform allows construction of a wide range of luminal diameters and muscular layer thicknesses, thus providing a toolbox to create variable anatomy. In this device, lymphatic muscle cells align circumferentially while endothelial cells aligned axially under flow, as only observed in vivo in the past. This system successfully characterizes the dynamics of cell size, density, growth, alignment, and intercellular gap due to co-culture and shear. Finally, exposure to pro-inflammatory cytokines reveals that the device could facilitate the regulation of endothelial barrier function through the lymphatic muscle cells. Therefore, this bioengineered platform is suitable for use in preclinical research of lymphatic and blood mechanobiology, inflammation, and translational outcomes.

Received 14th August 2021, Accepted 23rd November 2021

DOI: 10.1039/d1lc00720c

rsc.li/loc

1. Introduction

Lymphatics, as a one-way transport system, plays a crucial role in the human body, collecting interstitial fluid and proteins and returning them to blood circulation. Besides, lymphatic vessels carry out the significant tasks of immune cell trafficking and lipid absorption. Despite their vital role in maintaining body homeostasis and initiating numerous conditions such as cancer metastasis, lymphatic vascular physiology remains understudied relative to the blood vasculature.2-4 While several in vivo and ex vivo animal models exist and have contributed to some significant discoveries in the field,5,6 they can lack predictive power. Also, there are relatively few multicellular in vitro models of

lymphatic vessels that include relevant cell-cell interactions. Microfluidic models of blood and lymphatic vessels are emerging, which provides an enormous opportunity to fill this gap. Still, the ones that exist mostly focus on characterizing lymphatic endothelial permeability,7-11 tumorlymphatic interactions, 12-16 and lymphangiogenesis, 17,18 and none of these devices have included lymphatic muscle cells yet. A lymphangion is the functional unit of lymphatics, containing two major cell components: lymphatic muscle cells (LMCs) and lymphatic endothelial cells (LECs). 19 LMCs are crucial in lymphatics, as they lead to efficient drainage, luminal flow, and pressure regulation.20 Dysfunction of the lymphatic muscle may contribute to the development of pathologies such as lymphedema, for which there is no available cure. 21,22 Conversely, the secretion of mediators from LECs under various shear stress conditions has been shown to regulate muscle tissue.²³ However, existing tools lack the suitable cylindrical microenvironment for cells to experience in vivo physiological stress and strain conditions. 7,15,16 For example, the morphology and alignment of LMCs play a significant role in their function and molecular response.²⁴ Based on in vivo observations, LMCs can be found packed in a relatively thin muscle layer while

^a Department of Biomedical Engineering, College of Engineering, Texas A&M University, 101 Bizzell Street College Station, TX, 77843, USA. E-mail: a.jain@tamu.edu; Fax: +979 845 4450; Tel: +979 845 5532

^b Department of Medical Physiology, College of Medicine, Texas A&M Health Science Center, Bryan, TX, USA

^c Department of Cardiovascular Sciences, Houston Methodist Academic Institute, Houston, TX, USA

[†] Electronic supplementary information (ESI) available. See DOI: 10.1039/ d1lc00720c

Lab on a Chip Paper

maintaining a uniform density around the endothelium at each vessel's cross-section. However, the current fabrication techniques to obtain 3D vasculature models result in either an asymmetrical²⁸⁻³⁰ or relatively thick and nonphysiological ECM layer^{12,31} surrounding the lumen. Similarly, the LEC-LMC crosstalk is known to play a significant role in lymphatic function and this LEC-LMC signaling can be due to mechanical or inflammatory cues. 32,33 Although the effect of physical forces on LEC alignment and LMC remodeling has been studied individually, 24,34 there remains a need to study the LEC-LMC signaling under mechanical and inflammatory conditions in a representative model.

Here, we engineered the first 3D cylindrical lymphangionon-chip (lymphangion-chip) consisting of the co-culture of LECs and LMCs within an extracellular matrix for several days under fluid shear (Fig. 1). With a fabrication technique specifically developed to wrap LMCs uniformly around the LECs, we showed that both LMCs and LECs maintain their essential phenotype, growth and subendothelial characteristics, and morphological alignment, as either seen or expected in vivo. We then characterized the sensitivity of co-cultured LECs and LMCs due to shear and inflammatory cues. Overall, the data suggest that the lymphangion-chip will serve as an experimental model for preclinical lymphatic (and blood) vascular research and pharmacological testing.

2. Results

2.1 Design and engineering of the lymphangion-chip

We were inspired to create the lymphangion-chip as a platform technology offering control over geometry, mechanical properties, and fluid dynamics relevant to the diversity of lymphangions in vivo. Importantly, our aim was to create a cylindrical/elliptical microfluidic organ-chip consisting of a monoculture of LECs surrounded by multiple layers of uniformly thick LMCs embedded inside collagen hydrogel as an initial supporting ECM. While several lumen forming techniques exist in the literature, ^{28,31,35-43} there are very few that can be easily be made cylindrical or elliptical and can also support culture of the muscle cells in an in vivo like morphology. In particular, the viscous finger patterning method has now been adopted several times to make microfluidic endothelialized lumens, 28,44,45 but in co-culture settings, this method has not demonstrated a uniform distribution of wrapped muscle cells around endothelium. This technique is believed to rely primarily on viscous fingering (also known as Saffman-Taylor instability) that is a fluid dynamics phenomenon in which a less viscous fluid (cell medium) flows through and displaces a more viscous liquid (liquid collagen), creating finger-shaped structures. We hypothesized that in this technique, convective fluid dynamics characteristics - fluid pressure head across the inlet and outlet of the microfluidic channel and gravity - also determine the size and position of the lumens than solely liquid displacement due to the differences in the two fluids' viscosities.

To test this hypothesis, we perfused an LMC-hydrogel mixture into the device by attaching an inlet reservoir, and producing vacuum inside the channel using a syringe connected to the outlet, either when the device is placed horizontally on the incubator rack (classical viscous fingering method) or when it is rotated by 90° to align the channel's axis with the gravitational direction (gravitational lumen patterning or GLP). While keeping the device in this position, the less viscous fluid (cell medium) displaced the highly viscous fluid (collagen-LMC mixture) and formed a lumen (Fig. 2A). When the GLP method was adopted, the thickness of the ECM was relatively conserved in different angular positions around the inner hollow cavity, as observed by

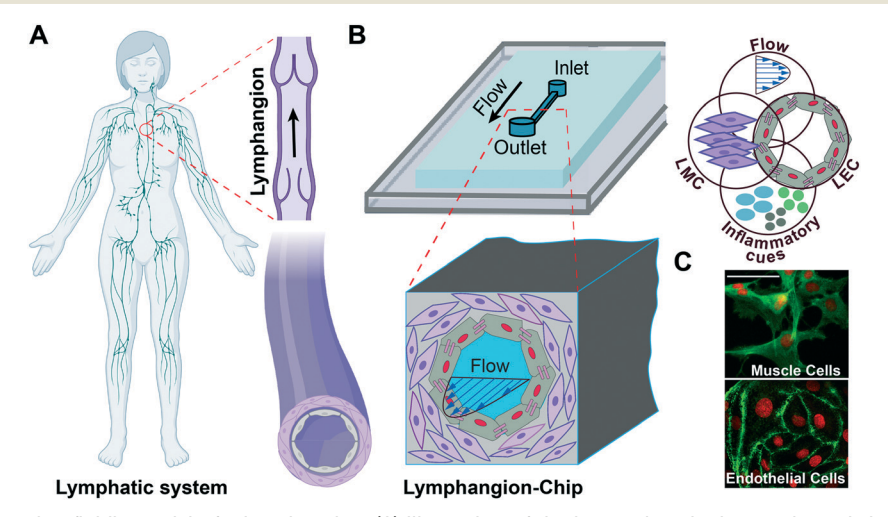


Fig. 1 Lymphangion-chip: microfluidic model of a lymphangion. (A) Illustration of the human lymphatic vessel consisting a lymphangion which is the unit between the two adjacent valves and (B) an engineering drawing of the lymphangion-chip with co-cultures of lymphatic endothelial cells (LECs) and lymphatic muscle cells (LMCs) that is leveraged to analyze the responses to flow and inflammatory cues. (C) A representative confocal image set of on-chip LMCs (green: F-actin) and LECs (green: VE-cadherin) under co-culture conditions. Scale bar: 50 µm.

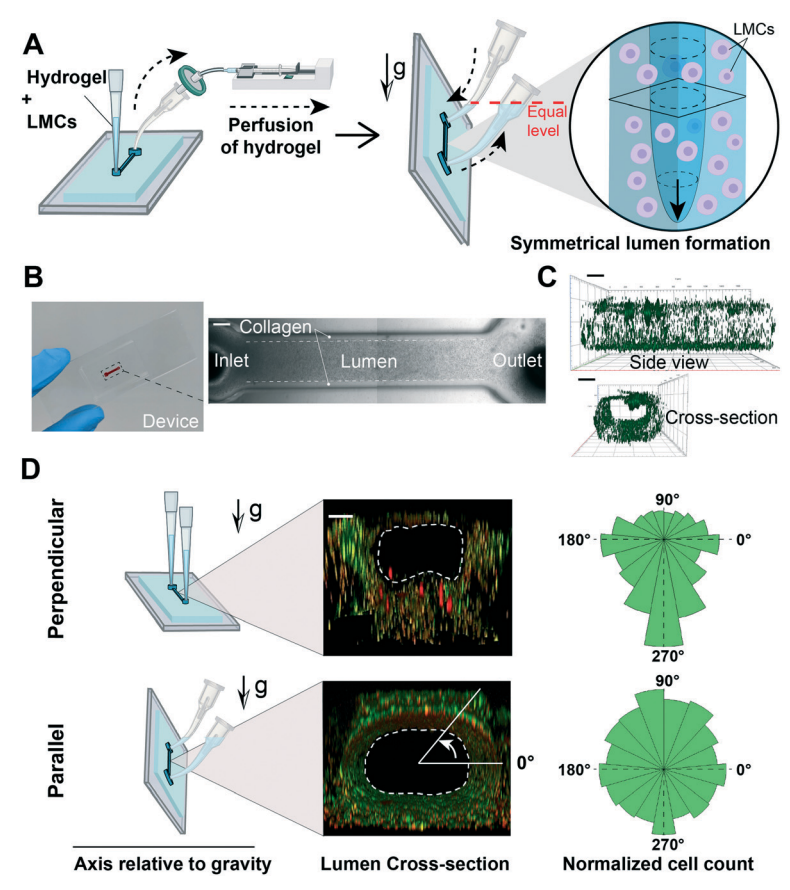


Fig. 2 Gravitational lumen patterning (GLP) technique to fabricate the lymphangion-chip. (A) The LMC-matrix mixture was perfused into the device by producing vacuum using a syringe connected to the outlet. Then, the devices were rotated by 90° (vertical position) so that the microfluidic channel aligned parallel to the direction of gravity. While keeping the device in the vertical position, a curved tip filled with LMC medium was added to the inlet while rotating the outlet tip so that both tips share a horizontal plane (equal level) for the cell medium not to flow out of the device. In this case, the less viscous fluid (cell medium) would wash away the highly viscous fluid (hydrogel) and form a 3D symmetrical lumen. (B) The fabricated device containing the lumen formed by GLP. (C) Side and cross-section views of the 3D lumen (green: fluorescent beads adhered to the collagen surface demonstrating the lumen boundary). (D) Effect of gravity on lumen symmetry when the device axis is perpendicular or parallel to the gravity direction. Scale bars: 200 μ m; n = 3 for the experiment.

doping the matrix with fluorescent beads (Fig. 2B and C) or by directly visualizing the LMCs within the matrix (Fig. 2D). This relatively uniform distribution was absent when we adopted the classical viscous fingering technique. We suspect that due to the buoyancy effect, the higher density fluid (collagen) tends to displace the lower density liquid (cell medium) and push it up toward the top of the channel, thus resulting in a variably thick ECM around the lumen. However, by keeping devices vertically and hence, aligning the gravitational force in the vessel's axial direction, we prevented this transverse effect of buoyant force and established a 3D lumen with a nearly symmetrical crosssection.

Then, we used the GLP technique to build lymphangionchips of variable sizes and ECM thicknesses. By changing the hydrostatic pressure at the chip inlet (140 to 340 Pa) while performing GLP, we could modulate the lumen diameter from a range of 400 µm to 800 µm (Fig. 3A and B). Also, since the collagen concentration is directly proportional to its viscosity and hydraulic resistance, we found that increasing the collagen concentration from 3 to 5 mg ml⁻¹ (\sim 60%) during GLP resulted in a 30% lumen size reduction (Fig. 3C and D). We also altered the outer lumen diameter (i.e., the vessel's thickness) by manufacturing molds with 600, 400, and 200 µm channel widths and confirmed that lumen formation using GLP was successful in this range as well (Fig. 3E). Taken together, these results show that mechanical factors, such as the hydrostatic pressure, microchannel size, and gravitational effect, as well as our supporting biomaterial - collagen concentration - can be varied to create hollow lumens of a wide range of sizes, thicknesses, and interstitial mechanical properties relevant to lymphatic vessels.

2.2 Reconstitution of lymphatic endothelial and muscle tissues in the lymphangion-chip

Since the endothelial and muscle cells are the two main tissue components of a lymphatic vessel, 46 we set out to confirm if we can co-culture these two lymphatic cell types in

B A Lumen Diameter (μm 800 600 400 µm 400 750 µm 850 µm 200 140 290 340 140 Pa 340 Pa Hydrostatic Pressure (Pa) D **€** 800 Lumen Diameter (650 um 580 µm Collagen (mg/ml) E

Fig. 3 Engineering and tuning of the lymphangion-chip. (A) Graph and (B) representative images of engineering the lumen inner diameter and the muscle tissue thickness by setting the hydrostatic pressure and (C and D) collagen concentration. (E) Engineering the outer vessel diameter by running the GLP method in chips with various channel widths (200-600 µm) (mixture of green fluorescent beads with cell medium specifies the lumen). All scale bars: 200 μ m; *p < 0.05, **p < 0.005, ****p < 0.0001; n = 3-5 for all the experiments.

400 μm

our GLP microfluidic constructs using just one cell culture medium formulation. In the beginning, we seeded only LECs on the luminal side of the chip and found that LECs formed a monolayer of confluent endothelial cells with properly formed cell-cell junctions in nearly two days. Using cell specific culture medium, LECs stayed confluent even after five days, and barrier integrity was maintained (Fig. 4A). In the next experiment, LMCs alone were mixed with collagen and perfused within the device. After five days of monoculture using the medium specified for this cell, we found that LMCs formed multilayers of oval-shaped structures embedded inside the collagen matrix, similar to the observed in vivo morphology.^{25,26} We evaluated the distribution and proliferation and confirmed the presence of LMCs all over the lumen (Fig. 4B). Next, to identify the standard cell culture conditions for a successful co-culture, we investigated the effect of environmental CO₂ percentage and cell medium combination on LMC and LEC growth, respectively. We observed that even though LECs reached full confluency in all combinations of LEC: LMC medium, a CO₂ of 5% and LEC:LMC ratios of 1:0 and 3:1 resulted in 100% cell coverage in less than 60 hours. In contrast, LMCs were more sensitive to LEC: LMC medium for which only LEC: LMC ratios of 1:0 and 1:3 resulted in 100% confluency (Fig. 4C and D). Based on these datasets, we identified that a

CO₂ of 5% and LEC:LMC medium ratio of 1:3 may be suitable for the co-culture. Using the derived formulation, a mixture of LMCs and collagen was perfused in the device, followed by lumen formation via the GLP technique. After one day, LECs were seeded through the lumen on the collagen face and were kept in the incubator. Confocal fluorescence microscopy analysis revealed that a confluent layer of endothelium surrounded by multiple layers of muscle cells was formed on-chip (Fig. 4E). In co-cultured devices, the average lumen inner diameter and muscle layer thickness are measured to be nearly 750 µm and 150 µm, respectively. These images provide the first evidence of a successful lymphatic vessel-on-chip consisting of both LECs and LMCs cultured together using a common medium formulation.

200 μm

To assess the physiological relevance of the LEC and LMC interface, we examined the on-chip endothelium and muscle layer gap as well as cell growth in co-culture versus monoculture conditions. The gap between LEC and LMC layers stayed nearly uniform under LMC monoculture, but it reduced steadily over time and reached nearly 5 µm in 4 days after LEC-LMC co-culture (Fig. 5A-C). Thus, LMCs respond and migrate toward LECs resulting in a time-dependent decrease in the subendothelial gap that is consistent with prior in vivo and in vitro observations for vascular cells.⁴⁷ Correspondingly, our observation of on-chip cell culture over

Lymphatic muscle cells

LMC culture

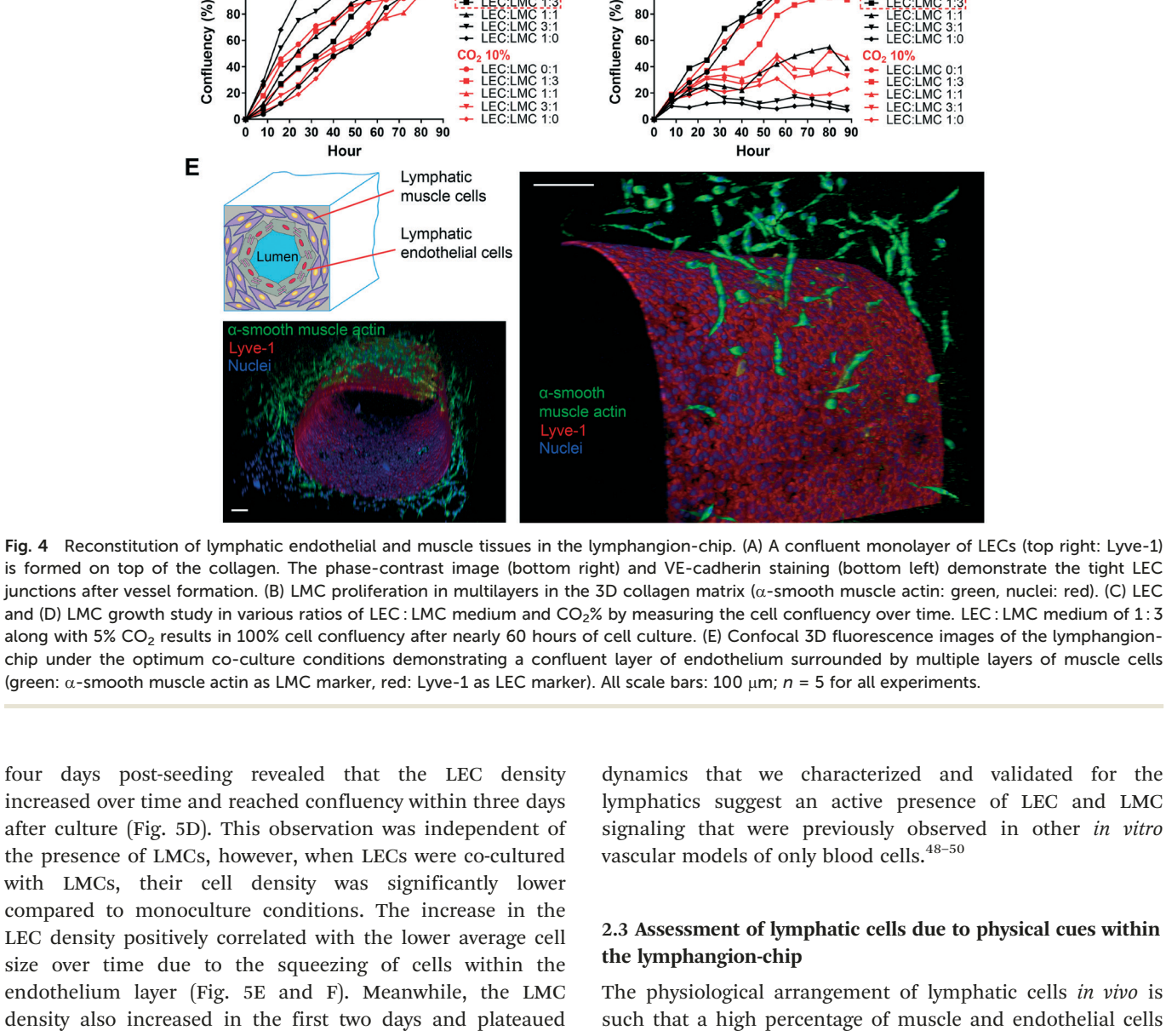
10 20 30 40 50 60 70 80 90

A

Collagen VE-cadherin

C

100



Lymphatic endothelial cells

LEC culture

B

D

100

80

60 40

dynamics that we characterized and validated for the lymphatics suggest an active presence of LEC and LMC signaling that were previously observed in other in vitro vascular models of only blood cells. 48-50

2.3 Assessment of lymphatic cells due to physical cues within the lymphangion-chip

The physiological arrangement of lymphatic cells in vivo is such that a high percentage of muscle and endothelial cells align perpendicular and parallel to the vessel's axial direction, respectively. 25,51-54 We speculated that this cell alignment - LMCs perpendicular to axially aligned LECs -

after, with no particularly significant difference between

monoculture vs. co-culture with LECs at the end of 5 days (Fig. 5G and H). These on-chip LEC and LMC growth

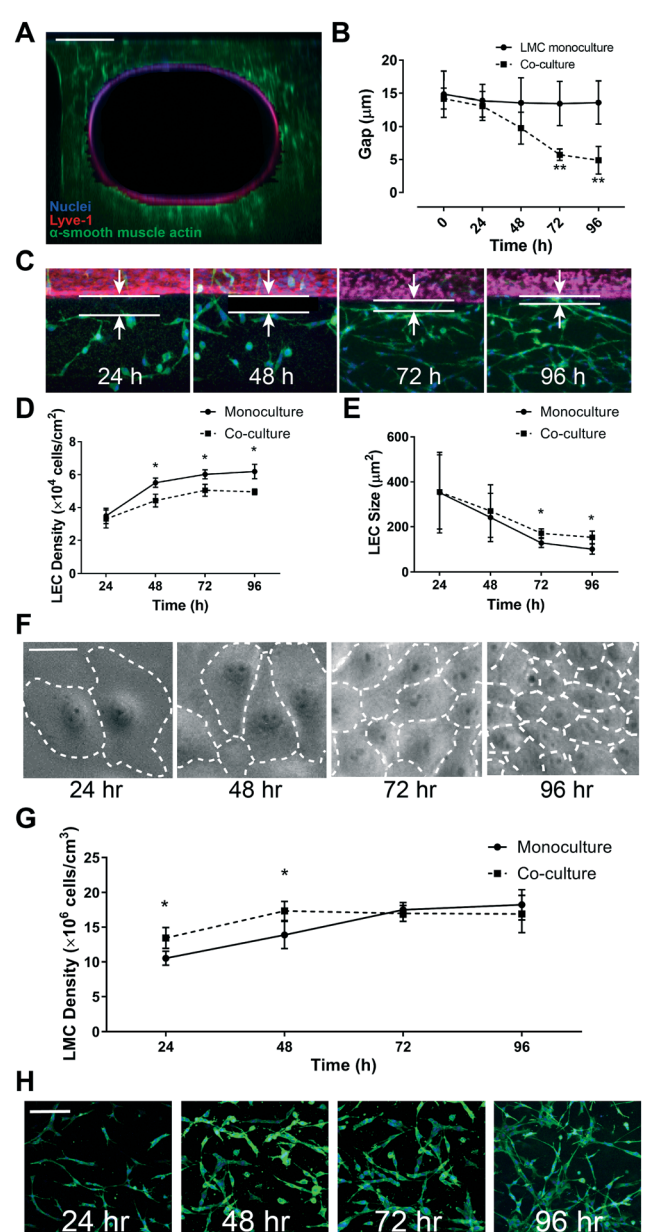


Fig. 5 Assessment of lymphatic endothelial and muscle cells within the lymphangion-chip. (A) Confocal cross-sectional image showing LECs (red) surrounded by LMCs (green); scale bar: 200 μm. (B) The average gap distance between endothelium and muscle layers over 96 hours after cell culture, shown graphically, and (C) via representative images of LECs (red) and LMCs (green); scale bar: 20 μm. (D) LMC density and (E) size vs. time either in monoculture (solid line) or coculture with LMCs (dotted line). (F) Representative images of LECs showing an increase in cell density and decrease in cell size when cultured on-chip; scale bar: 50 µm. (G) Graph and (H) representative images of LMC (green) density in the 3D ECM in monoculture versus co-culture; scale bar: 50 μ m; *p < 0.05, **p < 0.005; n = 5–7 for all experiments.

will be facilitated by the co-culture of LECs with LMCs. To test this, we compared the lymphatic cell orientation in coculture versus monoculture within the chip. We prepared three sets of devices containing: only LMCs, only LECs, and

LMC-LEC co-culture. After five days of monoculture, we found that LMCs aligned mostly axially in all lumen sections (sides, top, and bottom). However, co-cultured with LECs, were circumferentially oriented LMCs perpendicular to the axial vessel direction) (Fig. 6A). Further, when we exposed the LEC-LMC co-culture to a typical physiological shear (1 dyne cm⁻²),⁵⁵ we found a significantly more axial alignment of LECs and circumferential alignment of LMCs, relative to static culture conditions (Fig. S1†). The LEC alignment in the flow direction within the lymphangionchip matches the previous in vitro studies for endothelial cells. 54,56-58 Interestingly, when we applied an intermediate shear (0.1 dyne cm⁻²) representative of the lymphedema condition in which the lymphatic system's blockage prevents efficient lymph drainage, 59,60 we observed a relatively poor axial alignment of LECs and circumferential alignment of LMCs. Also, regardless of the shear, co-culturing muscle cells with endothelial cells always produced a relatively more axial orientation of LECs and circumferential orientation of LMCs, strengthening the device's capability to include active signaling between the two cell types (Fig. 6B-D).

2.4 Evaluation of lymphatic endothelial barrier function due to inflammatory cues within the lymphangion-chip

Several studies support the role of inflammatory cytokines, including TNF-α, in endothelial dysfunction and increased permeability.⁶¹ TNF-α is known to decrease lymphatic contractility⁶² and disrupt the lymphatic endothelial barrier function. 63 Since the in vitro effect of TNF- α on LEC-LMC co-culture has not been characterized before, we finally set out to illustrate the power of the lymphangionchip as a tool to systematically investigate how LMCs could regulate LEC function under the influence of inflammatory signals. First, to characterize the lymphatic endothelial permeability, we measured the diffusion of fluorescein isothiocyanate (FITC)-dextran,64 and found that dextran may diffuse through lymphatic endothelial cells as a function of its molecular weight (Fig. 7A and B). The vessel permeability for 4 kDa molecules $(3 \times 10^{-5} \text{ cm s}^{-1})$ was significantly larger than that for 20 and 70 kDa conjugates ($<5 \times 10^{-6}$ cm s⁻¹) (Fig. 7C). These results confirm that the lymphangion-chip's endothelium is leakier for small molecules compared to larger molecules that possess the size of albumin (~68 kDa), supported by observations made in animal models.65 Next, when we exposed the lymphangion-chip to TNF-α either when LECs and LMCs were cultured alone or together, we found a significant increase in permeability relative to our untreated controls. However, when LMCs were co-cultured with LECs, we discovered that the lymphatic endothelial barrier function was relatively conserved, suggesting its influence in maintaining tissue homeostasis (Fig. 7D). The specific signaling pathways involved in LMC-induced recovery post-inflammation is an intriguing topic to study with our platform in the future.

Lab on a Chip

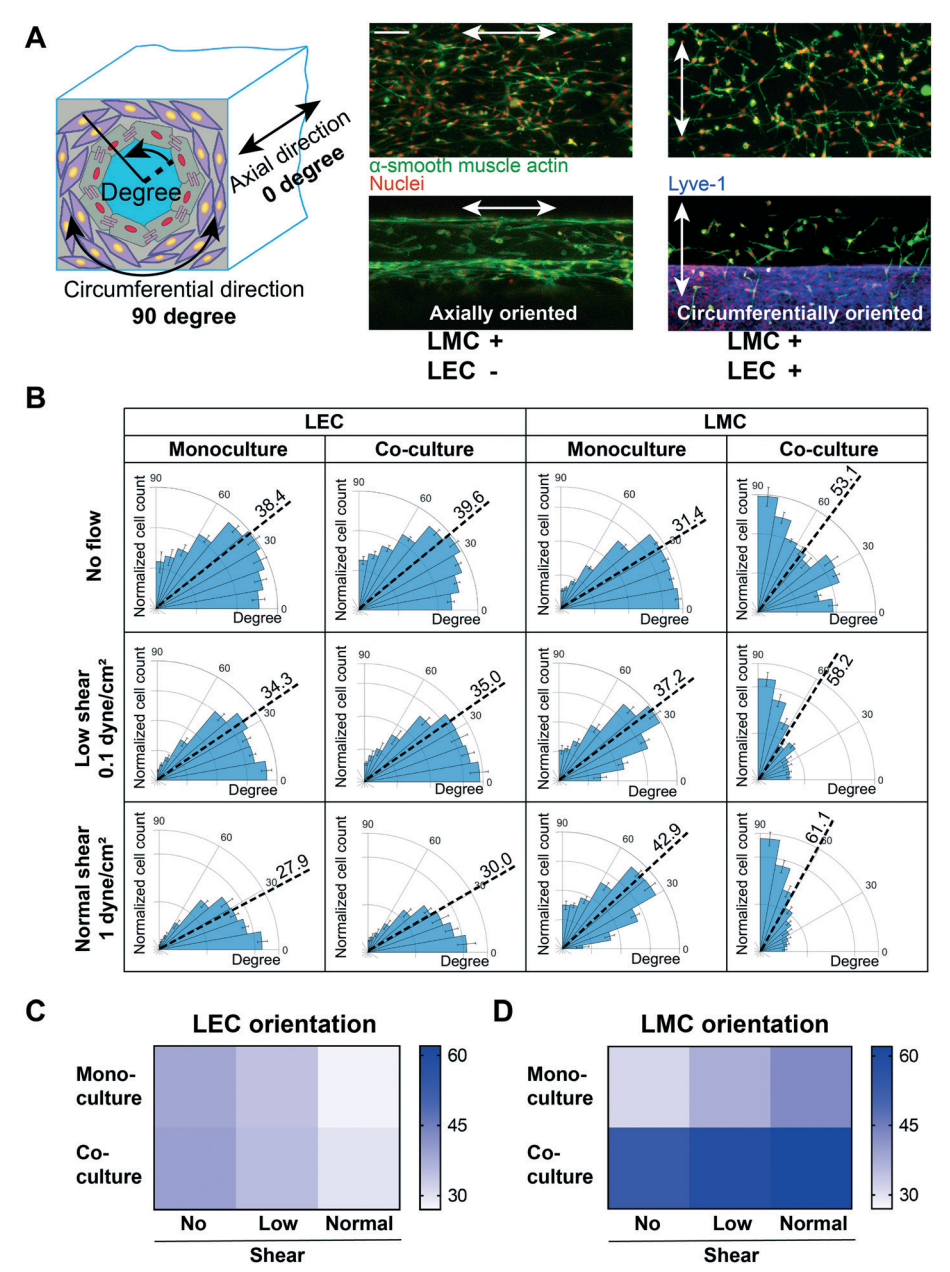


Fig. 6 Assessment of lymphatic cells due to physical cues within the lymphangion-chip. (A) LMC alignment under monoculture versus LEC-LMC co-culture conditions. LMCs (green) tend to orient mostly axially in monoculture. In contrast, co-cultured with LECs (red), LMCs align circumferentially which is closer to in vivo conditions (green: a-smooth muscle actin; red: Lyve-1). (B) The polar histograms of LEC and LMC alignment under three conditions: no flow, low shear, and normal shear. LMCs orient more circumferentially under normal shear conditions (i.e., higher shear rate) while LECs orient in the flow direction. Heatmaps of (C) LEC and (D) LMC mean orientation angle in monoculture and coculture while being exposed to no flow, low shear, or normal shear conditions. All scale bars: 200 μ m; n = 5 for all experiments.

3. Discussion

The endothelial and muscle cells are two key cell types that generate and regulate lymph flow in lymphatics and set the response to mechanical stimulation inflammation. 20,66,67 The normal interactions between these two cell types are important for the homeostasis of the lymphatic transport, and any aberrant interaction between them may lead to loss of junction integrity and flow.⁶⁸ But, this LEC-LMC signaling is not fully characterized in

experimental models, and the relatively few in vitro studies that exist have attempted to unveil the effects of mechanical forces only on LECs.⁶⁹ Several multicellular vascular organon-chip models have now been published and are currently being deployed in preclinical research and pharmaceutical discoveries, 70 including designs to co-culture endo/epithelial and smooth muscle cells in rectangular multichannels.71,72 Even though these models demonstrate vascular EC-SMC coculture and arterial function,71 the muscle layer is not wrapped circumferentially around the endothelium as seen

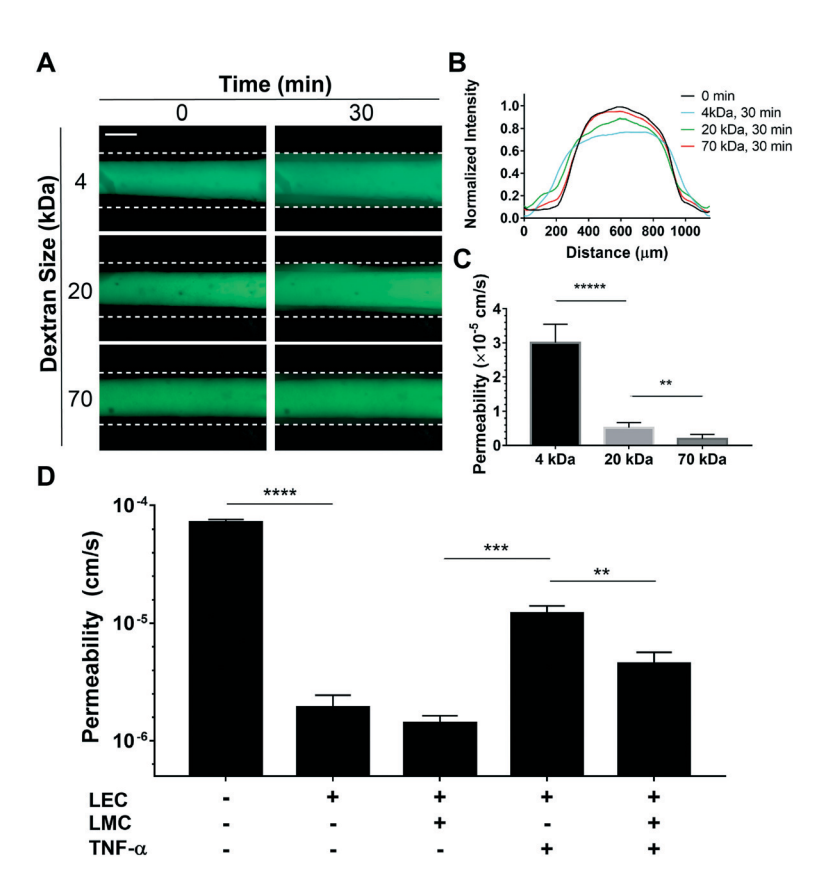


Fig. 7 Evaluation of lymphatic endothelial barrier function due to inflammatory cues within the lymphangion-chip. (A) Representative fluorescence images of FITC-dextran diffusion through the LEC monolayer. Two sets of images are captured from the vessel in 0 and 30 minutes after perfusing the FITC-dextran conjugates, shown in the left and right panels, respectively (green: fluorescent conjugates). (B) Normalized fluorescence intensity plot for different FITC-conjugate sizes within the lymphangion-chip. We plotted normalized Gaussian curves for 0 and 30 minutes after perfusion of three sizes of FITC-conjugates. (C) Measured permeability using the area under the curve for the lymphangion-chip. Smaller FITC-dextran conjugates perfuse easier through endothelial cell gaps, thus, resulting in larger permeability values. (D) Permeability for the lymphangion-chip made of only LECs and LEC-LMC co-culture before and after exposure to TNF- α as an inflammatory cytokine. TNF- α enhances the vessel permeability under both conditions leading to larger values of permeability. When co-cultured with LECs, LMCs help in partial recovery of endothelium permeability after inflammatory cytokine treatment. Scale bar: 200 μ m; *p < 0.005, ***p < 0.005, ***p < 0.001, ****p < 0.0001; n = 0.0015 for all experiments.

in vivo. Notably, there is currently no design to co-culture and study cell signaling between lymphatic endothelial and mural cells. Importantly, no studies have included the lymphatic muscle cells in their in vitro studies or culture them appropriately with the endothelium. To address this gap and enable prolonged LEC-LMC co-culture in a physiologically relevant environment, we created a 3D cylindrical lymphangion-chip through gravitational viscous finger patterning or GLP that harnesses the control of the buoyant effect and pressure difference across the channel not done before in prior designs. Our results show that this platform affords flexibility in determining the physical geometrical parameters of a lymphangion. By fabricating the lymphangion-chip with the GLP method, we offer a toolbox to alter the lumen's inner and outer diameter as well as the muscle tissue stiffness and thickness in a robust and physiologically-relevant manner. 19,53,73,74 Therefore, engineered tunable platform may also guide future studies beyond what we present here and can be leveraged in studying other types of vascular tissues.

Our observation of a time-dependent decrease in the subendothelial gap strongly suggests proactive LEC-LMC signaling as LECs and LMCs grow and proliferate within the device. The growth factors released by endothelial cells, such as polypeptide platelet-derived growth factor-B (PDGF-B), 47,75 may produce a concentration gradient around the endothelial layer, promoting the proliferation and migration of LMCs toward the endothelium layer, via their surface receptors, such as tyrosine kinase receptor PDGFR-β. 75,76 Future studies may allow such a hypothesis to be effectively tested with our platform. Also, proliferative smooth muscle cells are known to inhibit endothelial cell proliferation. 48,77 Within the lymphangion-chip, we saw a similar growth pattern, and the LEC growth rate was inhibited under co-culture conditions. The mechanisms that regulate such lymphatic endothelialmuscle cell crosstalk are beyond the scope of this work; however, this platform can be used for such studies without a significant need for animal models.

Since our approach produces a symmetrical and cylindrical lumen surrounded by a matrix, we could coLab on a Chip Paper

culture LECs and LMCs to align in the axial and circumferential direction, respectively, as frequently observed in vivo. Our device further demonstrated a robust sensitivity of this relative alignment of the two cells with respect to the presence or absence of co-culture and mechanical forces (shear stress), thus suggesting that LECs and LMCs are biologically and functionally active within the chip.

The lymphatic vasculature is essential in modulating the inflammatory response by altering interstitial fluid extravasation and drainage. During inflammation, the lymphatic vessel experiences a significant enlargement in inflamed tissue leading to an elevation in vessel leakiness and thus losing its full functionality.78 Studying LEC shown that endothelium monolayer integrity has permeability increases in response to inflammatory stimuli. 63 However, the effect of LMCs in cytokine-induced hyperpermeability of the endothelium is largely unknown. The lymphangion-chip revealed the possibility of the contribution of LMCs to partial recovery of endothelial barrier function after exposure to TNF-α. Although our absolute permeability measurements are typically higher than those quantified for ex vivo animal models, likely due to the difference in methodology, cell type, etc., 79,80 the trends we have obtained are fairly consistent with other reports of in vitro lymphatic vascular models. 11 While detailed signaling analysis of LMCs in barrier function recovery is beyond the scope of this study, we expect that the lymphangion-chip can be used to assess the clinical relevance and consequences of such LEC-LMC crosstalk in subsequent studies.

Our lymphangion-chip has not reached its full potential. For example, there is an opportunity to include pericytes in the model. Also, even though we introduced shear uniformly, in the collecting lymphatics, flow and pressure are uniquely pulsatile in nature.⁵¹ It may be critical to introduce such flow profiles for some future studies that investigate lymphatic mechanobiology. Also, lymphatic vessels exhibit phasic and tonic contractility in most murine models, if not all, 81 but we did not focus on that in this work. Although pacemaker cells are believed to initiate lymphatic phasic contractions, prior studies suggest that external stimulation (for example, by including electrical energy) may also be needed to initiate such contractile activity in vitro. 82,83 Some prior literature also suggests that these cells may partially maintain their tonic contractions in the 3D matrix.⁸⁴ Thus, the lymphangion-chip can potentially be used to characterize muscle tonic contractile behavior that can be more directly characterized in future studies. Finally, LMCs and LECs in this project are derived from rat mesenteric vessels and human dermal tissue, respectively. This is a limitation because human LMCs are not commercially available.

4. Conclusion

In summary, this organ-chip technology allows us to include essential lymphatic vascular components in a tunable 3D physiological environment. We can easily dissect and control

several variables such as flow, geometry, chemical cues, etc., that impact LECs and LMCs in a way that may potentially result in a translational impact. This platform can be immediately combined with molecular and gene analysis tools to provide more precise insight into the regulatory signaling mechanisms of lymphatic vascular physiology/ pathophysiology and drug treatments. Finally, the platform can also be applied in blood vascular models.

Experimental section/methods

5.1 Lymphangion-chip design and fabrication

The microfluidic channels of the platform were designed using SolidWorks (900 µm wide, 900 µm high, 5 mm long, 1.5 mm diameter inlet reservoir, 2 mm diameter outlet reservoir) and were subsequently 3D printed on VeroWhite resin using an Eden350 setup to make the mold. Then, the microfluidic devices were fabricated by soft lithography of polydimethylsiloxane (PDMS, Dow Corning). Briefly, the base and cross-linker were mixed at a 10:1 ratio, and then the mold was filled with the PDMS mixture and cured at 80 °C for 2 hours. Later, the PDMS slab was removed from the master mold, and the inlets and outlets were punched with a 1 mm biopsy punch (Ted Pella). Finally, the PDMS slabs containing the channel features were plasma bonded to a PDMS-coated glass slide using a 100 watts plasma cleaner (Thierry Zepto, Diener Electronics), and devices were kept at 80 °C for 30 minutes to enhance the binding. The detailed protocol is published elsewhere.85

5.2 Device pretreatment and gravitational lumen patterning

The devices were pretreated before hydrogel perfusion to enhance the collagen-PDMS bonding strength using a previously described protocol.86 In brief, the devices were plasma treated and silanized immediately by filling with 10% v/v silane ((3-aminopropyl)trimethoxysilane, Sigma-Aldrich) in ethanol. After 15 minutes of incubation at room temperature, the channels were washed extensively with ethanol and kept in an 80° oven for 2 hours to dry. Then, the devices were filled with 2.5% v/v glutaraldehyde (Sigma-Aldrich) and were kept at room temperature for 15 minutes. Finally, the microfluidic devices were washed multiple times with ethanol and kept in the 80° oven for 2 hours (Fig. S2A†).

The devices were first degassed in a vacuum chamber for two hours and then filled with an ice-cold high concentration hydrogel-LMC mixture (see the next section) using the vacuum produced by connecting syringes to the outlets (Fig. S2B†). Then, the inlet tips were removed and the devices were rotated by 90° to align the microfluidic channels parallel to the gravity direction (vertical position). Later while the devices were kept vertically, additional curved tips filled with 50 µl of ice-cold cell medium were released at the inlets. In the vertical position, the curved tips were both facing upward so as to share a horizontal line to force stop cell medium flow after lumen formation (Fig. S2B†). After observing the cell medium flow from the inlets to the outlets, the devices were placed in a 37° incubator while their position was fixed either vertically using clips. The tips were removed gently after 7 minutes to avoid collagen-plastic tip adhesion, and the devices were turned back again to the horizontal position. The tips were replaced with cell medium droplets to prevent air bubble formation in device inlets and outlets. After 30 minutes of incubation, the devices were removed from the incubator, and fresh syringe tips were added gently to the inlets and outlets (Fig. S2C†). At this point, the collagen was already polymerized, and the 3D lumen could be observed using a phase-contrast microscope. Next, the devices were washed substantially but gently with the cell medium. To achieve this, each time, only 50 µl of warm cell medium was added to the inlet tips while the excessive solution was removed from the outlet tips. This process was repeated multiple times resulting in the passive pumping of the cell medium within the lumen to wash away all the chemical solution remaining within the ECM (Fig. S2D†).

5.3 Lymphatic cell culture

We employed a previously published technique to isolate endothelial cells and muscle cells from the rat mesenteric lymphatic vessel.87-89 In summary, after isolation of rat mesenteric collecting lymphatics, the vessel was cleaned and incubated on a gelatin-coated plastic culture dish. Highglucose Dulbecco's modified Eagle's medium supplemented with 20% FBS, 2 mM sodium pyruvate, 2 mM L-glutamine, and antibiotics was added to the dish to promote the growth of LMCs. Then, the vessel was removed after migration of the muscle cells out of the vessel's cut sections (after 3-4 days). In this step, LMCs can be recognized by their morphology and also by the negative uptake of fluorescent acetylated-LDL which is taken up specifically by endothelial cells via the "scavenger cell pathway" of LDL metabolism.90 If some colonies of LECs were observed in culture, they were eliminated physically with a rubber policeman or by laser ablation using a UV laser microscope. Finally, LMCs were allowed to grow further and then were trypsinized and passaged after 7-10 days. The used protocols for rat cell isolation were approved by the Texas A&M University Laboratory Animal Care Committee (IACUC 2019-0284). The human dermal LECs were purchased commercially (Promocell). All cells were cultured separately in standard cell culture flasks featuring vacuum-gas plasma tissue culture treatment (ThermoFisher Scientific) and were passaged after reaching 90% cell confluency (passage 4-7). LECs were maintained with 99% v/v Endothelial Cell Growth Medium MV2 (full supplemental kit, PromoCell) and 1% v/v antibiotic cocktail (Gibco) in a humidified 37° and 5% CO2 incubator, while LMCs were kept in 89% v/v DMEM/F-12 (Gibco), 10% v/ v FBS (Gibco) and 1% v/v antibiotic cocktail in a 10% CO2

To achieve on-chip 3D cell culture, LMCs were first trypsinized and resuspended in 33 µl DMEM/F12 and then extensively mixed with a solution of 110 µl high

concentration rat tail type I collagen (9 mg ml⁻¹, Corning), 40 μl HEPES (1 M, Gibco), 14 μl sodium bicarbonate (NaHCO₃, 1 M, ThermoFisher Scientific), and 3 µl sodium hydroxide (NaOH, 1 M, ThermoFisher Scientific) with a final concentration of 5×10^6 cells per ml. The cell-gel mixture was then used in the GILP process to form the 3D lumen (described previously). The devices were kept for one day before seeding LECs, while the LMC medium was exchanged twice a day. Next, LECs were seeded using the previously described method with modifications. 91 In summary, endothelial cells were trypsinized and added to the co-culture medium (1:3 LEC:LMC medium, see Results) with a final concentration of 2.5×10^6 cells per ml. Then, the devices were filled with the cell suspension and were incubated in a 5% CO₂ incubator for 40 minutes for the cells to adhere fully to collagen. After flushing the unadhered cells using the fresh medium, the devices were turned upside down, and this same process was repeated four times for each side of the lumen (Fig. S3D†). The co-culture medium was exchanged twice a day, each 15 minutes, for devices under no-flow conditions. For flow experiments, the devices were connected to a programmable syringe pump (Harvard) to apply a constant and continuous flow rate that resulted in the average wall shear stress measured in the rat mesenteric lymphatic vessel (~1 dyne cm⁻²).^{55,92} To model lymphedemalike conditions (i.e., inadequate lymph drainage and inflammation), the flow rate was reduced by 10-fold, resulting in ~ 0.1 dyne cm⁻² wall shear stress.

5.4 Immunohistochemistry

Immunohistochemistry of lymphangion-chip devices was measured with standard fixation (4% paraformaldehyde, Sigma), permeabilization (0.5% Triton X-100, Sigma), and blocking (10% bovine serum albumin, ThermoFisher Scientific) methods. Fixed devices were later incubated with mouse or rabbit primary antibodies, including α -smooth muscle actin (a-SMA, eBioscience), vascular endothelialcadherin (VE-cadherin, Invitrogen), or lymphatic vessel endothelial hyaluronan receptor 1 (LYVE1, Invitrogen) followed by secondary anti-mouse or anti-rabbit fluorescent antibodies (Invitrogen). Finally, cell nuclei were stained with Hoechst 33258 (Invitrogen).

5.5 Cell functional assessment

To evaluate on-plate and on-chip cell density and confluency, we used the non-invasive and non-destructive method described before.93 Quantification of cell alignment was performed using OrientationJ, a Fiji software plug-in for directional image analysis based on evaluating gradient structure tensors. 94,95 The OrientationJ software code was used to characterize the orientation and isotropic properties of a region of interest in an image, based on the evaluation of the structure tensor in a local neighborhood.⁹⁶ To employ this method, LECs and LMCs were fixed and stained with Hoechst and α-SMA, respectively.³⁴ Then, z-stack confocal

Lab on a Chip Paper

images of the devices were taken to capture all cells within the vessels. All images were bandpass filtered using highand low-frequency cut-offs at 2 and 20 pixels. Finally, images were post-processed to obtain the tensor containing angle θ of cell alignment with respect to the axial direction by analyzing nuclei and actin orientation. Finally, the distribution of cell alignment was plotted in a polar histogram. In order to measure the gap size between endothelium and muscle tissues, orthogonal views of the 3D confocal images of devices were plotted and then the average distance between the nearest LMCs and the endothelium layer for the whole device was measured and plotted in each time-point.

5.6 Inflammatory cytokine treatment

The cytokine treatment started after four days of endothelial cell culture to ensure the formation of a confluent intact endothelium layer. After removing the cell medium and replacing it with the phenol-free experimental medium, we waited for 2 hours for cells to stabilize. Then, 50 µl medium containing TNF- α (10 ng ml $^{-1}$, recombinant from *E. coli*, Sigma) was added to the devices. ^{63,97,98} After 2 hours, 50 μl of cell medium mixed with FITC labeled BSA was added to the vessels, and fluorescence images were taken immediately and after 30 minutes.

5.7 Endothelial permeability measurement

To measure vessel permeability, 50 µl of 1 µM working concentration of dextran solution (Texas Red dextran, 4 kDa, 20 kDa, and 70 kDa, ThermoFisher Scientific) in the phenolred free medium was added to the device inlet while aspirating the experimental medium of the device outlet. Therefore, the fluid within the inlet and outlet reservoirs reached the same elevation quickly to minimize the flow and pressure increase inside the vessel. The solute transport inside the vessel was then measured immediately and after 30 minutes of diffusion. We plotted the fluorescence intensity in three vertical lines along the vessel length. The vessel-onchip permeability coefficient was calculated using eqn (1):99

$$P = \left(\frac{1}{I_0}\right) \left(\frac{I_{\rm f} - I_0}{t_{\rm f} - t_0}\right) \left(\frac{D}{4}\right) \tag{1}$$

where I_0 and I_f are the total florescence intensities outside the vessel at 0 and 30 minutes, respectively. I_0 and I_f were calculated by summing up the area under the curve for fluorescence intensities from the LEC monolayer to the channel wall. t_0 and t_f are the initial and final timepoints, and D is the vessel diameter.

5.8 Imaging and microscopy

Standard fluorescence and phase-contrast images were acquired using a Zeiss Axio Observer Z1 inverted setup (LD Plan Neofluar, 10×, NA 0.4) and Zeiss Axio Vert.A1 (DIC, Axiocam 503, 20×, Zeiss), respectively. Images were analysed and processed with ZEN 2.3 lite software (Zeiss). Z-stack and stitched confocal images were obtained with an Olympus FV1000 microscope. Live-cell images were captured with a CytoSMART 2 system.

5.9 Statistical analysis

Data and error bars are represented as the mean and standard error of the mean (SEM), respectively. Statistical analysis was performed using GraphPad Prism v7 (GraphPad Software Inc.). The comparison between data groups was carried out using Student's t-test, and a P value of less than 0.05 was considered statistically significant.

Author contributions

A. S. performed the microfluidics experiments. A. S. and A. J. analysed the results, made the figures, and wrote the paper with feedback from all the authors; T. F. performed the experiments to find the coculture conditions for LECs and LMCs used in this study; S. C., M. M and D. C. Z. isolated and characterized the lymphatic muscle cells used in this study, and M. M and D. C. Z. also contributed to data analysis.

Conflicts of interest

The authors declare no conflict of interest.

Acknowledgements

We thank Dr. S. Vitha at the Microscopy and Imaging Center at Texas A&M University for assisting with confocal imaging. Research reported in this publication was supported by the NIBIB R21EB025945, NSF CAREER Award number 1944322, Texas A&M Engineering; and President's Excellence in Research Funding Award of Texas A&M University to A. J.

References

- 1 M. A. Swartz, The physiology of the lymphatic system, Adv. Drug Delivery Rev., 2001, 50(1-2), 3-20.
- 2 S. G. Rockson, Lymphedema, Am. J. Med., 2001, 110(4),
- 3 S. A. Stacker, S. P. Williams, T. Karnezis, R. Shayan, S. B. Fox and M. G. Achen, Lymphangiogenesis and lymphatic vessel remodelling in cancer, Nat. Rev. Cancer, 2014, 14(3), 159-172.
- 4 R. Paduch, The role of lymphangiogenesis and angiogenesis in tumor metastasis, Cell. Oncol., 2016, 39(5), 397-410.
- 5 R. Hadrian and D. Palmes, Animal Models of Secondary Lymphedema: New Approaches in the Search for Therapeutic Options, Lymphatic Res. Biol., 2017, 15(1), 2-16.
- 6 W. S. Shin and S. G. Rockson, Animal models for the molecular and mechanistic study of lymphatic biology and disease, Ann. N. Y. Acad. Sci., 2008, 1131(1), 50-74.
- 7 M. Sato, N. Sasaki, M. Ato, S. Hirakawa, K. Sato and K. Sato, Microcirculation-on-a-chip: A microfluidic platform for assaying blood-and lymphatic-vessel permeability, PLoS One, 2015, **10**(9), e0137301.

- 8 G. M. Price, K. M. Chrobak and J. Tien, Effect of cyclic AMP on barrier function of human lymphatic microvascular tubes, *Microvasc. Res.*, 2008, 76(1), 46–51.
- 9 R. L. Thompson, E. A. Margolis, T. J. Ryan, B. J. Coisman, G. M. Price, K. H. Wong and J. Tien, Design principles for lymphatic drainage of fluid and solutes from collagen scaffolds, *J. Biomed. Mater. Res., Part A*, 2018, **106**(1), 106–114.
- 10 K. H. Wong, J. G. Truslow, A. H. Khankhel, K. L. Chan and J. Tien, Artificial lymphatic drainage systems for vascularized microfluidic scaffolds, *J. Biomed. Mater. Res.*, Part A, 2013, 101(8), 2181–2190.
- 11 M. M. Gong, K. M. Lugo-Cintron, B. R. White, S. C. Kerr, P. M. Harari and D. J. Beebe, Human organotypic lymphatic vessel model elucidates microenvironment-dependent signaling and barrier function, *Biomaterials*, 2019, 214, 119225.
- 12 J. M. Ayuso, M. M. Gong, M. C. Skala, P. M. Harari and D. J. Beebe, Human Tumor-Lymphatic Microfluidic Model Reveals Differential Conditioning of Lymphatic Vessels by Breast Cancer Cells, *Adv. Healthcare Mater.*, 2020, 9(3), 1900925.
- 13 K. M. Lugo-Cintrón, J. M. Ayuso, B. R. White, P. M. Harari, S. M. Ponik, D. J. Beebe, M. M. Gong and M. Virumbrales-Muñoz, Matrix density drives 3D organotypic lymphatic vessel activation in a microfluidic model of the breast tumor microenvironment, *Lab Chip*, 2020, 20(9), 1586–1600.
- 14 X. Cao, R. Ashfaq, F. Cheng, S. Maharjan, J. Li, G. Ying, S. Hassan, H. Xiao, K. Yue and Y. S. Zhang, A tumor-on-a-chip system with bioprinted blood and lymphatic vessel pair, *Adv. Funct. Mater.*, 2019, 29(31), 1807173.
- 15 B. Kwak, A. Ozcelikkale, C. S. Shin, K. Park and B. Han, Simulation of complex transport of nanoparticles around a tumor using tumor-microenvironment-on-chip, *J. Controlled Release*, 2014, 194, 157–167.
- 16 M. Pisano, V. Triacca, K. Barbee and M. Swartz, An in vitro model of the tumor-lymphatic microenvironment with simultaneous transendothelial and luminal flows reveals mechanisms of flow enhanced invasion, *Integr. Biol.*, 2015, 7(5), 525–533.
- 17 D. Choi, E. Park, E. Jung, Y. J. Seong, J. Yoo, E. Lee, M. Hong, S. Lee, H. Ishida and J. Burford, Laminar flow downregulates Notch activity to promote lymphatic sprouting, J. Clin. Invest., 2017, 127(4), 1225–1240.
- 18 S. Kim, M. Chung and N. L. Jeon, Three-dimensional biomimetic model to reconstitute sprouting lymphangiogenesis in vitro, *Biomaterials*, 2016, **78**, 115–128.
- 19 K. P. Arkill, J. Moger and C. P. Winlove, The structure and mechanical properties of collecting lymphatic vessels: an investigation using multimodal nonlinear microscopy, *J. Anat.*, 2010, 216(5), 547–555.
- 20 P. Y. von der Weid and D. C. Zawieja, Lymphatic smooth muscle: the motor unit of lymph drainage, *Int. J. Biochem. Cell Biol.*, 2004, **36**(7), 1147–1153.
- 21 L. Kaiser, M. Mupanomunda and J. F. Williams, Brugia pahangi-induced contractility of bovine mesenteric lymphatics studied in vitro: A role for filarial factors in the

- development of lymphedema?, Am. J. Trop. Med. Hyg., 1996, 54(4), 386-390.
- 22 J. P. Scallan, S. D. Zawieja, J. A. Castorena-Gonzalez and M. J. Davis, Lymphatic pumping: mechanics, mechanisms and malfunction, *J. Physiol.*, 2016, 594(20), 5749–5768.
- 23 J. A. Castorena-Gonzalez, S. D. Zawieja, M. Li, R. S. Srinivasan, A. M. Simon, C. de Wit, R. de la Torre, L. A. Martinez-Lemus, G. W. Hennig and M. J. Davis, Mechanisms of connexin-related lymphedema: a critical role for Cx45, but not Cx43 or Cx47, in the entrainment of spontaneous lymphatic contractions, *Circ. Res.*, 2018, 123(8), 964–985.
- 24 J. S. Hooks, C. C. Clement, H. D. Nguyen, L. Santambrogio and J. B. Dixon, In vitro model reveals a role for mechanical stretch in the remodeling response of lymphatic muscle cells, *Microcirculation*, 2019, 26(1), e12512.
- 25 M. S. Razavi, J. Leonard-Duke, B. Hardie, J. B. Dixon and R. L. Gleason, Axial stretch regulates rat tail collecting lymphatic vessel contractions, *Sci. Rep.*, 2020, 10(1), 1–11.
- 26 Y. Ohtani and O. Ohtani, Postnatal development of lymphatic vessels and their smooth muscle cells in the rat diaphragm: a confocal microscopic study, *Arch. Histol. Cytol.*, 2001, 64(5), 513–522.
- 27 E. A. Bridenbaugh, I. T. Nizamutdinova, D. Jupiter, T. Nagai, S. Thangaswamy, V. Chatterjee and A. A. Gashev, Lymphatic muscle cells in rat mesenteric lymphatic vessels of various ages, *Lymphatic Res. Biol.*, 2013, 11(1), 35–42.
- 28 L. L. Bischel, S. H. Lee and D. J. Beebe, A practical method for patterning lumens through ECM hydrogels via viscous finger patterning, J. Lab. Autom., 2012, 17(2), 96–103.
- 29 M. N. de Graaf, A. Cochrane, F. E. van den Hil, W. Buijsman, A. D. van der Meer, A. van den Berg, C. L. Mummery and V. V. Orlova, Scalable microphysiological system to model threedimensional blood vessels, APL Bioeng., 2019, 3(2), 026105.
- 30 A. Herland, A. D. van der Meer, E. A. FitzGerald, T. E. Park, J. J. Sleeboom and D. E. Ingber, Distinct Contributions of Astrocytes and Pericytes to Neuroinflammation Identified in a 3D Human Blood-Brain Barrier on a Chip, *PLoS One*, 2016, 11(3), e0150360.
- 31 J. A. Jiménez-Torres, S. L. Peery, K. E. Sung and D. J. Beebe, LumeNEXT: a practical method to pattern luminal structures in ECM gels, *Adv. Healthcare Mater.*, 2016, 5(2), 198–204.
- 32 S. Lutter, S. Xie, F. Tatin and T. Makinen, Smooth muscle-endothelial cell communication activates Reelin signaling and regulates lymphatic vessel formation, *J. Cell Biol.*, 2012, **197**(6), 837–849.
- 33 E. J. Behringer, J. P. Scallan, M. Jafarnejad, J. A. Castorena-Gonzalez, S. D. Zawieja, J. E. Moore, M. J. Davis and S. S. Segal, Calcium and electrical dynamics in lymphatic endothelium, *J. Physiol.*, 2017, 595(24), 7347–7368.
- 34 E. Michalaki, V. N. Surya, G. G. Fuller and A. R. Dunn, Perpendicular alignment of lymphatic endothelial cells in response to spatial gradients in wall shear stress, *Commun. Biol.*, 2020, 3(1), 1–9.
- 35 L. Andrique, G. Recher, K. Alessandri, N. Pujol, M. Feyeux, P. Bon, L. Cognet, P. Nassoy and A. Bikfalvi, A model of guided

- cell self-organization for rapid and spontaneous formation of functional vessels, Sci. Adv., 2019, 5(6), eaau6562.
- 36 H. Lee, S. Kim, M. Chung, J. H. Kim and N. L. Jeon, A bioengineered array of 3D microvessels for vascular permeability assay, Microvasc. Res., 2014, 91, 90-98.
- 37 W. J. Polacheck, M. L. Kutys, J. Yang, J. Eyckmans, Y. Wu, H. Vasavada, K. K. Hirschi and C. S. Chen, A non-canonical Notch complex regulates adherens iunctions and vascular barrier function, Nature, 2017, 552(7684), 258-262.
- 38 J. W. Song and L. L. Munn, Fluid forces control endothelial sprouting, Proc. Natl. Acad. Sci. U. S. A., 2011, 108(37), 15342-15347.
- 39 D.-H. T. Nguyen, S. C. Stapleton, M. T. Yang, S. S. Cha, C. K. Choi, P. A. Galie and C. S. Chen, Biomimetic model to reconstitute angiogenic sprouting morphogenesis in vitro, Proc. Natl. Acad. Sci. U. S. A., 2013, 110(17), 6712-6717.
- 40 C. Mandrycky, B. Hadland and Y. Zheng, 3D curvatureinstructed endothelial flow response vascularization, Sci. Adv., 2020, 6(38), eabb3629.
- 41 S. G. Rayner, K. T. Phong, J. Xue, D. Lih, S. J. Shankland, E. J. Kelly, J. Himmelfarb and Y. Zheng, Reconstructing the human renal vascular-tubular unit in vitro, Adv. Healthcare Mater., 2018, 7(23), 1801120.
- 42 K. A. Heintz, M. E. Bregenzer, J. L. Mantle, K. H. Lee, J. L. West and J. H. Slater, Fabrication of 3D biomimetic microfluidic networks in hydrogels, Adv. Healthcare Mater., 2016, 5(17), 2153-2160.
- 43 N. V. Menon, C. Su, K. T. Pang, Z. J. Phua, H. M. Tay, R. Dalan, X. Wang, K. H. H. Li and H. W. Hou, Recapitulating atherogenic flow disturbances and vascular inflammation in a perfusable 3D stenosis model, Biofabrication, 2020, 12(4), 045009.
- 44 J. Chin, Lattice Boltzmann simulation of the flow of binary immiscible fluids with different viscosities using the Shan-Chen microscopic interaction model, Philos. Trans. R. Soc., A, 2002, 360(1792), 547-558.
- 45 L. L. Bischel, E. W. Young, B. R. Mader and D. J. Beebe, Tubeless microfluidic angiogenesis assay with threedimensional endothelial-lined microvessels, Biomaterials, 2013, 34(5), 1471-1477.
- 46 I. Rusznyák, M. Földi and G. Szabó, Lymphatics and lymph circulation: physiology and pathology, Elsevier, 2013.
- K. Gaengel, G. Genové, A. Armulik and C. Betsholtz, Endothelial-mural cell signaling in vascular development and angiogenesis, Arterioscler., Thromb., Vasc. 2009, 29(5), 630-638.
- 48 M. D. Lavender, Z. Pang, C. S. Wallace, L. E. Niklason and G. A. Truskey, A system for the direct co-culture of endothelium on smooth muscle cells, Biomaterials, 2005, 26(22), 4642-4653.
- 49 H. Yoshida, M. Nakamura, S. Makita and K. Hiramori, Paracrine effect of human vascular endothelial cells on human vascular smooth muscle cell proliferation: transmembrane co-culture method, Heart Vessels, 1996, 11(5), 229-233.

- 50 J. H. Campbell and G. R. Campbell, Endothelial cell influences on vascular smooth muscle phenotype, Annu. Rev. Physiol., 1986, 48(1), 295-306.
- 51 J. E. Moore Jr and C. D. Bertram, Lymphatic System Flows, Annu. Rev. Fluid Mech., 2018, 50(1), 459-482.
- 52 P. Y. Von Der Weid, Lymphatic vessel pumping and inflammation-the role of spontaneous constrictions and underlying electrical pacemaker potentials, Pharmacol. Ther., 2001, 15(8), 1115-1129.
- 53 T. Ohhashi, T. Azuma and M. Sakaguchi, Active and passive mechanical characteristics of bovine mesenteric lymphatics, Am. J. Physiol., 1980, 239(1), H88-H95.
- 54 D. Choi, E. Park, E. Jung, Y. J. Seong, M. Hong, S. Lee, J. Burford, G. Gyarmati, J. Peti-Peterdi and S. Srikanth, ORAI1 activates proliferation of lymphatic endothelial cells in response to laminar flow through Krüppel-like factors 2 and 4, Circ. Res., 2017, 120(9), 1426-1439.
- 55 J. B. Dixon, S. T. Greiner, A. A. Gashev, G. L. Cote, J. E. Moore and D. C. Zawieja, Lymph flow, shear stress, and lymphocyte velocity in rat mesenteric prenodal lymphatics, Microcirculation, 2006, 13(7), 597-610.
- 56 T. Osaki, T. Kakegawa, T. Kageyama, J. Enomoto, T. Nittami and J. Fukuda, Acceleration of vascular sprouting from fabricated perfusable vascular-like structures, PLoS One, 2015, 10(4), e0123735.
- 57 Y.-G. Park, J. Choi, H.-K. Jung, I. K. Song, Y. Shin, S.-Y. Park and J.-W. Seol, Fluid shear stress regulates vascular remodeling via VEGFR-3 activation, although independently of its ligand, VEGF-C, in the uterus during pregnancy, Int. J. Mol. Med., 2017, 40(4), 1210-1216.
- Y. Yang, B. Cha, Z. Y. Motawe, R. S. Srinivasan and J. P. Scallan, VE-cadherin is required for lymphatic valve formation and maintenance, Cell Rep., 2019, 28(9), 2397-2412. e4.
- 59 P. S. Mortimer, The pathophysiology of lymphedema, Cancer, 1998, 83(S12B), 2798-2802.
- A. Stanton, R. Mellor, G. Cook, W. Svensson, A. Peters, J. Levick and P. Mortimer, Impairment of lymph drainage in subfascial compartment of forearm in breast cancer-related lymphedema, Lymphatic Res. Biol., 2003, 1(2), 121-132.
- 61 C. Zhang, The role of inflammatory cytokines in endothelial dysfunction, Basic Res. Cardiol., 2008, 103(5), 398-406.
- 62 Y. X. Chen, S. Rehal, S. Roizes, H.-L. Zhu, W. C. Cole and P.-Y. von der Weid, The pro-inflammatory cytokine TNF- α inhibits lymphatic pumping via activation of the NF-κB-iNOS signaling pathway, Microcirculation, 2017, 24(3), e12364.
- 63 W. E. Cromer, S. D. Zawieja, B. Tharakan, E. W. Childs, M. K. Newell and D. C. Zawieja, The effects of inflammatory cytokines on lymphatic endothelial barrier function, Angiogenesis, 2014, 17(2), 395-406.
- 64 R. Natarajan, N. Northrop and B. Yamamoto, Fluorescein Isothiocyanate (FITC)-Dextran Extravasation as a Measure of Blood-Brain Barrier Permeability, Curr. Protoc. Neurosci., 2017, **79**(1), 9.58.1.
- 65 N. Ono, R. Mizuno and T. Ohhashi, Effective permeability of hydrophilic substances through walls of lymph vessels: roles

of endothelial barrier, Am. J. Physiol., 2005, 289(4), H1676-H1682.

- 66 D. C. Zawieja, Lymphatic microcirculation, *Microcirculation*, 1996, 3(2), 241–243.
- 67 A. A. Gashev, Lymphatic vessels: pressure- and flow-dependent regulatory reactions, *Ann. N. Y. Acad. Sci.*, 2008, **1131**, 100–109.
- 68 P. Saharinen, T. Tammela, M. J. Karkkainen and K. Alitalo, Lymphatic vasculature: development, molecular regulation and role in tumor metastasis and inflammation, *Trends Immunol.*, 2004, 25(7), 387–395.
- 69 K. N. Margaris and R. A. Black, Modelling the lymphatic system: challenges and opportunities, *J. R. Soc., Interface*, 2012, 9(69), 601–612.
- 70 K. Gold, A. K. Gaharwar and A. Jain, Emerging trends in multiscale modeling of vascular pathophysiology: Organ-ona-chip and 3D printing, *Biomaterials*, 2019, 196, 2–17.
- 71 C. Su, N. V. Menon, X. Xu, Y. R. Teo, H. Cao, R. Dalan, C. Y. Tay and H. W. Hou, A novel human arterial wall-on-a-chip to study endothelial inflammation and vascular smooth muscle cell migration in early atherosclerosis, *Lab Chip*, 2021, 21(12), 2359–2371.
- 72 M. Humayun, C.-W. Chow and E. W. Young, Microfluidic lung airway-on-a-chip with arrayable suspended gels for studying epithelial and smooth muscle cell interactions, *Lab Chip*, 2018, 18(9), 1298–1309.
- 73 X. Deng, G. Marinov, Y. Marois and R. Guidoin, Mechanical characteristics of the canine thoracic duct: what are the driving forces of the lymph flow?, *Biorheology*, 1999, 36(5, 6), 391–399.
- 74 A. J. MacDonald, K. P. Arkill, G. R. Tabor, N. G. McHale and C. P. Winlove, Modeling flow in collecting lymphatic vessels: one-dimensional flow through a series of contractile elements, Am. J. Physiol., 2008, 295(1), H305–H313.
- 75 J. Andrae, R. Gallini and C. Betsholtz, Role of plateletderived growth factors in physiology and medicine, *Genes Dev.*, 2008, 22(10), 1276–1312.
- 76 J. Donovan, D. Abraham and J. Norman, Platelet-derived growth factor signaling in mesenchymal cells, *Front. Biosci.*, 2013, 18(1), 106–119.
- 77 T. Ziegler, R. W. Alexander and R. M. Nerem, An endothelial cell-smooth muscle cell co-culture model for use in the investigation of flow effects on vascular biology, *Ann. Biomed. Eng.*, 1995, 23(3), 216–225.
- 78 S. Schwager and M. Detmar, Inflammation and lymphatic function, *Front. Immunol.*, 2019, **10**, 308.
- 79 J. P. Scallan and V. H. Huxley, In vivo determination of collecting lymphatic vessel permeability to albumin: a role for lymphatics in exchange, *J. Physiol.*, 2010, 588(1), 243–254.
- 80 M. Jannaway and J. P. Scallan, VE-Cadherin and Vesicles Differentially Regulate Lymphatic Vascular Permeability to Solutes of Various Sizes, Front. Physiol., 2021, 12, 1553.
- 81 A. A. Gashev, M. J. Davis, O. Y. Gasheva, Z. V. Nepiushchikh, W. Wang, P. Dougherty, K. A. Kelly, S. Cai, P.-Y. Von Der Weid and M. Muthuchamy, Methods for lymphatic vessel culture and gene transfection, *Microcirculation*, 2009, **16**(7), 615–628.

- 82 T. J. Akl, G. L. Coté, Z. V. Nepiyushchikh, A. A. Gashev and D. C. Zawieja, Measuring contraction propagation and localizing pacemaker cells using high speed video microscopy, J. Biomed. Opt., 2011, 16(2), 026016.
- 83 B. O. Hald, J. A. Castorena-Gonzalez, S. D. Zawieja, P. Gui and M. J. Davis, Electrical communication in lymphangions, *Biophys. J.*, 2018, **115**(5), 936–949.
- 84 M. Al-Kofahi, F. Becker, F. Gavins, M. Woolard, I. Tsunoda, Y. Wang, D. Ostanin, D. Zawieja, M. Muthuchamy and P. von der Weid, IL-1β reduces tonic contraction of mesenteric lymphatic muscle cells, with the involvement of cycloxygenase-2 and prostaglandin E 2, *Br. J. Pharmacol.*, 2015, 172(16), 4038–4051.
- 85 A. Jain, T. Mathur, N. K. Pandian and A. Selahi, Organ-on-achip and 3D printing as preclinical models for medical research and practice, in *Precision Medicine for Investigators*, *Practitioners and Providers*, Elsevier, 2020, pp. 83–95.
- 86 D. Kim and A. E. Herr, Protein immobilization techniques for microfluidic assays, *Biomicrofluidics*, 2013, 7(4), 041501.
- 87 H. Hayes, E. Kossmann, E. Wilson, C. Meininger and D. Zawieja, Development and characterization of endothelial cells from rat microlymphatics, *Lymphatic Res. Biol.*, 2003, **1**(2), 101–119.
- 88 M. Muthuchamy, A. Gashev, N. Boswell, N. Dawson and D. Zawieja, Molecular and functional analyses of the contractile apparatus in lymphatic muscle, *FASEB J.*, 2003, 17(8), 920–922.
- 89 X. Zhang, S. Chakraborty, M. Muthuchamy and D. C. Zawieja, Isolation of Lymphatic Muscle Cells (LMCsLymphatic muscle cells (LMCs)) from Rat Mesentery, in *Cardiovascular Development: Methods and Protocols*, ed. X. Peng and W. E. Zimmer, Springer US, New York, NY, 2021, pp. 137–141.
- 90 J. C. Voyta, D. P. Via, C. E. Butterfield and B. R. Zetter, Identification and isolation of endothelial cells based on their increased uptake of acetylated-low density lipoprotein, *J. Cell Biol.*, 1984, 99(6), 2034–2040.
- 91 T. Mathur, K. A. Singh, N. K. Pandian, S.-H. Tsai, T. W. Hein, A. K. Gaharwar, J. M. Flanagan and A. Jain, Organ-on-chips made of blood: endothelial progenitor cells from blood reconstitute vascular thromboinflammation in vessel-chips, *Lab Chip*, 2019, **19**(15), 2500–2511.
- 92 T. J. Akl, T. Nagai, G. L. Coté and A. A. Gashev, Mesenteric lymph flow in adult and aged rats, *Am. J. Physiol.*, 2011, 301(5), H1828–H1840.
- 93 S. Busschots, S. O'Toole, J. J. O'Leary and B. Stordal, Non-invasive and non-destructive measurements of confluence in cultured adherent cell lines, *MethodsX*, 2015, 2, 8–13.
- 94 J. Schindelin, I. Arganda-Carreras, E. Frise, V. Kaynig, M. Longair, T. Pietzsch, S. Preibisch, C. Rueden, S. Saalfeld and B. Schmid, Fiji: an open-source platform for biological-image analysis, *Nat. Methods*, 2012, 9(7), 676–682.
- 95 Z. Püspöki, M. Storath, D. Sage and M. Unser, Transforms and operators for directional bioimage analysis: a survey, in *Focus on Bio-Image Informatics*, Springer, 2016, pp. 69–93.
- 96 R. Rezakhaniha, A. Agianniotis, J. T. C. Schrauwen, A. Griffa, D. Sage, C. V. Bouten, F. Van De Vosse, M. Unser and N. Stergiopulos, Experimental investigation of collagen

Lab on a Chip

- waviness and orientation in the arterial adventitia using confocal laser scanning microscopy, Biomech. Model. Mechanobiol., 2012, 11(3-4), 461-473.
- 97 G. Chaitanya, S. Franks, W. Cromer, S. Wells, M. Bienkowska, M. Jennings, A. Ruddell, T. Ando, Y. Wang and Y. Gu, Differential cytokine responses in human and mouse lymphatic endothelial cells to cytokines in vitro, Lymphatic Res. Biol., 2010, 8(3), 155-164.
- 98 K. Bove, P. Neumann, N. Gertzberg and A. Johnson, Role of ecNOS-derived NO in mediating TNF-induced endothelial barrier dysfunction, Am. J. Physiol., 2001, 280(5), L914-L922.
- 99 V. Huxley, F. Curry and R. Adamson, Quantitative fluorescence microscopy on single capillaries: alphalactalbumin transport, Am. J. Physiol., 1987, 252(1), H188-H197.